Effects of *Decyl*-aurachin D and Reversed Electron Transfer in Cytochrome *bd*†

Susanne Jünemann,‡ John M. Wrigglesworth,§ and Peter R. Rich*,‡

Glynn Research Institute, Bodmin, Cornwall PL30 4AU, U.K., and King's College London, Camden Hill Road, London W8 7AH, U.K.

Received January 10, 1997; Revised Manuscript Received June 2, 1997⊗

ABSTRACT: *Decyl*-aurachin D is a near-stoichiometric inhibitor of cytochrome *bd* from *Azotobacter vinelandii*. Interaction of *decyl*-aurachin D with the oxidase induces a redshift of the α-band and Soret band of a *b*-type cytochrome, probably *b*-558, suggesting close proximity of the inhibitor binding site to this haem and hence to the proposed quinol binding domain. The compound does not affect the oxygen binding site directly as judged from unchanged CO recombination kinetics to haem *d* in dithionite-reduced enzyme. Although in the presence of ubiquinol-1 a *decyl*-aurachin D containing sample generates levels of haem reduction and catalytic intermediates similar to the control, the approach to this steady state is severely inhibited. In addition to the spectral effect on *b*-558, *decyl*-aurachin D raises the midpoint potential of haem *b*-558, but also lowers that of haem *b*-595. Consistent with the shift in midpoint potentials, electron backflow from haem *d* to the *b*-type haems can be observed in *decyl*-aurachin D inhibited samples following photolysis of the mixed-valence CO-ligated form of the enzyme. The data show that *decyl*-aurachin D acts on the donor side of haem *b*-558 without substantially affecting internal electron transfer rates or the oxygen reduction site.

The cytochrome *bd* complex is a widely distributed bacterial ubiquinol oxidase.[1] It has been purified from a number of sources, including *Escherichia coli* (Miller & Gennis, 1983; Kita et al., 1984), *Photobacterium phosphoreum* (Konishi et al., 1986), *Klebsiella pneumoniae* (Smith et al., 1990), and *Azotobacter vinelandii* (Kolonay et al., 1994; Jünemann & Wrigglesworth, 1995), but most studies have been carried out on the enzymes from *E. coli* and *A. vinelandii*. The *A. vinelandii* and *E. coli* forms show close similarity with regard to genetic and spectral properties, immunological reactions, and enzyme kinetics (Kranz & Gennis, 1985a; Kelly et al., 1990a; Jünemann et al., 1995a). This is further reflected in a high degree of homology in the amino acid sequences as derived from the DNA sequences (Moshiri et al., 1991).

The oxidase comprises three haem redox centers, *b*-558, *b*-595, and *d*, but no copper. Haem *b*-558, ligated by His^{186} (*E. coli* numbering (Fang et al., 1989)) and Met^{393} (Kaysser et al., 1995; Spinner et al., 1995), is thought to be the primary electron acceptor from ubiquinol (Green et al., 1986). Haem *d* forms part of the oxygen binding site. The role of the third haem, *b*-595, which is high spin and pentacoordinate, is less clear, but it has been suggested that haems *b*-595 and *d* share a common binding pocket and may form a binuclear center (Hill et al., 1993; D'mello et al., 1994).

Specific inhibitors have long been a useful tool for probing structure−function relationships in the active centers of redox proteins. In the case of cytochrome *bd*, monoclonal antibodies have been used to localize an 11-amino acid sequence on subunit I of the *E. coli* enzyme, close to haem *b*-558, which is likely to form part of the quinol binding domain (Kranz & Gennis, 1984; Dueweke & Gennis, 1990). These findings were supported by limited proteolysis with trypsin or chymotrypsin which cleave subunit I at a single site close to the proposed quinol domain and lead to a loss of ubiquinol oxidase activity (Lorence et al., 1988; Dueweke & Gennis, 1991). However, neither treatment affected TMPD oxidation. Electron flow from ubiquinol to oxygen is also reported to be inhibited by a number of compounds known to affect Q-sites in other systems, including antimycin A, UHDBT, HQNO, and aurachins C and D (Miller & Gennis, 1983; Jünemann & Wrigglesworth, 1994; Meunier et al., 1995). Among these compounds, the aurachins, quinolone-type structures and natural products of the myxobacterium *Stigmatella aurantiaca* (Oettmeier et al., 1994), are of particular interest since they are the most powerful known inhibitors of the *E. coli bd* and *bo* type oxidases (Meunier et al., 1995). A number of 3-alkyl derivatives of aurachin D have been synthesized (Reil et al., 1994) and were shown to have potencies which are similar to those of the parent compound with membrane-bound cytochrome *bd* from *E. coli* (Meunier et al., 1995). Aurachin D and its derivatives act specifically on cytochrome *bd*, whereas aurachin C (the *N*-oxide of aurachin D) and its synthetic analogues are effective on both cytochrome *bd* and cytochrome *bo*.

We have used the effects of *decyl*-aurachin D on cytochrome *bd* from *A. vinelandii* in order to further characterize the structure and mechanism of this oxidase.

MATERIALS AND METHODS

Chemicals. *Decyl*-aurachin D (Reil et al., 1994) was provided by Prof. Walter Oettmeier. The compound was dissolved in ethanol and quantitated spectrophotometrically (in methanol) using an extinction coefficient at 240 nm of

† This work was supported by HFSP (grant ref RG-464/95M).

* Corresponding author. Tel./Fax: +171-380 7746. E-mail: prr@ucl.ac.uk.

‡ Glynn Research Institute. Present address: Department of Biology, University College London, Gower Street, London WC1E 6BT.

§ King's College London.

⊗ Abstract published in *Advance ACS Abstracts,* August 1, 1997.

[1] Abbreviations: DTT, dithiothreitol; *decyl*-aurachin D, 2-methyl-3-*n*-decyl-4(1*H*)-quinolone; HQNO, 2-*n*-heptyl-4-hydroxyquinoline *N*-oxide; TMPD, *N,N,N′,N′*-tetramethyl-*p*-phenylenediamine; UHDBT, 5-*n*-undecyl-6-hydroxy-4,7-dioxobenzothiazole.

S0006-2960(97)00055-X CCC: $14.00

25.8 mM^{-1} cm^{-1} (Walter Oettmeier, personal communication). Ubiquinone-1 was a gift from Prof. Richard Cammack. It was used as an ethanolic stock solution and quantitated from the borohydride-reduced *minus* oxidized spectrum using an extinction coefficient at 278 nm of 14.0 mM^{-1} cm^{-1} (Takamiya & Dutton, 1979). Duroquinol was prepared from the quinone as described previously (Rich, 1981). Stock solutions of up to 250 mM were made in dimethyl sulfoxide containing 10 mM HCl.

Organism, Bacterial Growth, and Preparation of Cytochrome bd. The cytochrome *bd* overproducing *A. vinelandii* strain MK8 (Kelly et al., 1990) was a kind gift of Prof. Robert Poole. Growth of cells and preparation of membranes were carried out as described by Kelly *et al.* (Kelly et al., 1990). The cytochrome *bd* complex was purified by the method of Jünemann & Wrigglesworth (Jünemann & Wrigglesworth, 1995).

Oxidase Activity. Oxidase activities were measured in a Clark-type oxygen electrode at 27 °C, containing 2.5 mL of 100 mM potassium phosphate, 1 mM EDTA, pH 7.9, and the substrate ubiquinone-1 plus 2 mM DTT. The reaction was started by adding 5−10 μg of cytochrome *bd* which had been preincubated for 5 min, on ice, in 10 μL of 0.1 M phosphate buffer, pH 7.9, containing 1 mM phospholipid (l-α-phosphatidylcholine from soybean, Type IV-S, Sigma).

Alternatively, duroquinol was used as a substrate in a medium containing 50 mM potassium phosphate, 1 mM EDTA, and 0.05% lauryl maltoside, pH 7.5. Duroquinol is a poor substrate for cytochrome *bd* with a turnover of around 50 O_2 s^{-1} at 1 mM duroquinol (pH 7.5), whereas the turnover number with ubiquinol-1 reaches a V_{max} of 1000 O_2 s^{-1} at pH 7.9 (Jünemann et al., 1995a) with about half this number at pH 7.5. Duroquinol was mostly used in optical experiments at micromolar *bd* concentrations to allow sufficient time for sample manipulation. As a further advantage, its use is not restrained by the rate limitation of quinol re-reduction, which is observed with the ubiquinol-1/DTT system at increased (>0.1 μM) *bd* levels. The preincubation step of cytochrome *bd* was omitted when duroquinol was used as substrate.

Spectrophotometric and Kinetic Measurements. Optical spectra and multiwavelength kinetics were monitored at room temperature in the same sample with a single-beam instrument built in house. *Decyl*-aurachin D binding spectra were recorded on a Varian Cary 210 spectrophotometer using a spectral band width of 1 nm and a scan rate of 2 nm s^{-1}. Substrates and media were as in oxygen electrode measurements.

Carbon monoxide was photolyzed from the dithionite-reduced, ligated form of the oxidase with a frequency-doubled Nd/YAG laser (Spectron Laser Systems, Rugby, U.K.). This provided a 10 ns pulse of light at 532 nm with an energy in excess of 100 mJ/pulse. Kinetic spectra were constructed from averaged transients taken cyclically at individual wavelengths.

Fast kinetics of internal electron redistribution in cytochrome *bd* were monitored following initiation of the reaction by flash photolysis of the one-electron-reduced, CO-ligated form of the enzyme. This was produced by addition of CO-saturated water to "as prepared" cytochrome *bd* in the presence of 3.5 mM glucose, 500 unit mL^{-1} catalase (from bovine liver, Sigma), and 100 units mL^{-1} glucose oxidase (from *Aspergillus niger*, Type X-2, Sigma) in 50 mM potassium phosphate, 1 mM EDTA, pH 7.5, in a sealed cuvette. Spectra were taken before the measurement to confirm quantitative formation of the CO-ligated species and after the experiment to check for any haem *b* reduction.

EPR Spectroscopy. Continuous-wave EPR spectra were recorded on a Bruker ESP300 spectrometer fitted with a TE103 rectangular cavity, a ∼9 GHz microwave source, a Hewlett-Packard microwave counter, and an Oxford Instruments liquid helium flow cryostat ESR900.

Redox Titrations. Conventional anaerobic redox titrations (Dutton & Wilson, 1974) of cytochrome *bd* (approximately 2 μM) were carried out under a nitrogen atmosphere in a medium containing 50 mM potassium phosphate, 2 mM EDTA, pH 7.5. Samples also included 3.5 mM glucose, glucose oxidase, and catalase, as described above. Redox potentials were measured in the stirred sample using a glassy carbon electrode and a Ag/AgCl reference electrode. Redox mediators were tetrachlorobenzoquinone (E_{m7} 340 mV), 1,2-naphthoquinone-4-sulfonate (210 mV), 1,2-naphthoquinone (145 mV), phenazine methosulfate (80 mV), and duroquinol (10 mV), all at 50 μM. The potential was varied with additions of sodium dithionite (100 mM stock) or potassium ferricyanide (50 mM stock). After stabilization of the potential, stirring was stopped and the spectrum between 500 and 700 nm was recorded. Titration curves for individual haems were derived from measurements using the following wavelengths: 562 nm (sample), 546 and 580 nm (references) for haem *b*-558; 596 nm (sample), 580 and 608 nm (references) for haem *b*-595; and 628 nm (sample), 608 and 660 nm (references) for haem *d*. The data represent points taken in both oxidative and reductive directions.

RESULTS

Determination of the Inhibitor Constant K_i. *Decyl*-aurachin D is a potent inhibitor of oxidase activity with ubiquinol-1 (plus DTT) as electron donor (Figure 1). Similar results were obtained with other quinol substrates such as duroquinol or with endogenous ubiquinol-8 *via* NADH or malate-sustained respiration (not shown). With TMPD (0.5 mM plus 10 mM ascorbate) as substrate, no inhibition was observed at *decyl*-aurachin D concentrations sufficient to inhibit quinol oxidation by about 95% (not shown).

A quantitative measure of inhibitor potency was obtained by titrating the ubiquinol-1 oxidase activity. *Decyl*-aurachin D shows very tight binding to the cytochrome *bd* complex, leading to inhibition at approximately stoichiometric amounts of inhibitor. Therefore, titration data were analyzed by procedures suggested by Dixon (Dixon, 1972) and Henderson (Henderson, 1972) for tightly binding inhibitors with one inhibitor binding site per protein (Figure 1). The inhibitor (dissociation) constant, K_i, for interaction of *decyl*-aurachin D with cytochrome *bd* from *A. vinelandii* was found to be 13 ± 3 nM. This value is 3 orders of magnitude lower than the K_i of other inhibitors likely to affect the quinol binding site such as antimycin A, UHDBT, or HQNO (K_i around 5−20 μM (Jünemann & Wrigglesworth, 1994)) and compares to a K_i close to 10 nM found for the inhibition of cytocrome *bd* from *E. coli* by *decyl*-aurachin D (Meunier et al., 1995).

The observed K_i was independent of ubiquinol-1 concentration. Similar findings with other membrane-bound, ubiquinol-dependent enzymes have been interpreted as

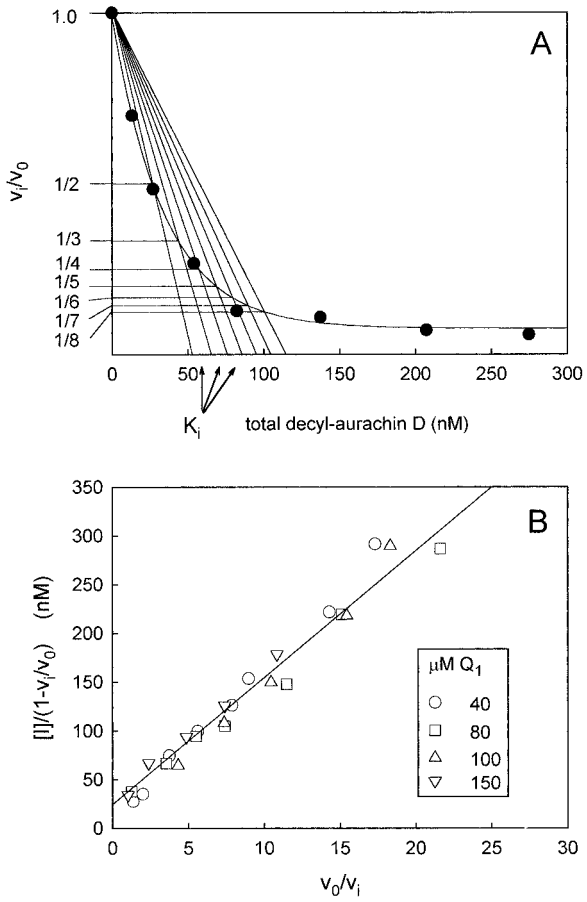

FIGURE 1: Inhibition of ubiquinol-1 oxidase activity by *decyl*-aurachin D. Rates of oxygen consumption by cytochrome *bd* (29 nM) were measured in 0.1 M potassium phosphate buffer, pH 7.9, at various concentrations of ubiquinol-1 plus 2 mM DTT. Cytochrome *bd* was preincubated with phospholipid as described in Methods. (A) Plot of fractional activity against inhibitor concentration at a selected ubiquinol-1 concentration (40 μM) with graphical analysis according to Dixon (1972). (B) Plot according to Henderson (1972). The slope gives the inhibitor constant K_i.

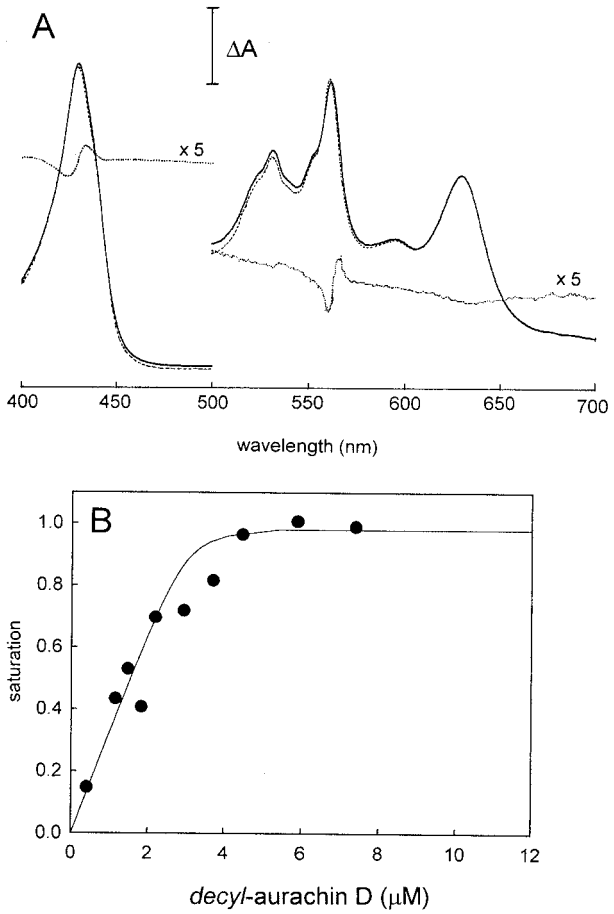

FIGURE 2: Spectral perturbations induced by *decyl*-aurachin D binding to cytochrome *bd*. (A) Purified, dithionite-reduced cytochrome *bd* (1.2 μM) in 0.1 M Hepes (pH 7). Absolute spectra reduced (—), plus 10 μM *decyl*-aurachin D (- - -) and difference spectrum (•••). The vertical bar represents $\Delta A = 0.015$ above 500 nm and $\Delta A = 0.1$ below 500 nm. (B) Titration of the *decyl*-aurachin D-induced red shift. Cytochrome *bd* (3 μM) in 0.1 M Hepes (pH 7) was reduced with dithionite. After addition of *decyl*-aurachin D from an ethanolic stock solutioin, the optical spectrum was recorded between 580 and 540 nm. The titration curve was constructed from the normalized absorbance difference at 565 *minus* 560 nm. Experimental data are overlayed with a calculated curve using $K_d = 46$ nM and 1.2 binding sites.

showing a noncompetitive mode of inhibition (e.g. Brandt et al. (1988), Friedrich et al. (1994), Musser et al. (1997)).

Spectral Effects of Decyl-aurachin D. As can be seen in Figure 2A, binding of *decyl*-aurachin D to dithionite-reduced cytochrome *bd* induces a red shift in the spectrum of one of the *b*-type haems, similar to the red shifts observed in the mitochondrial bc_1 complex with some inhibitors, e.g. antimycin A or myxothiazol (von Jagow & Link, 1986). This red shift could be titrated (Figure 2B) at inhibitor:cytochrome *bd* ratios comparable to those required in the oxygen electrode assays (Figure 1A). A K_d value of 46 nM with 1.2 binding sites was estimated using a standard binding equation (Bagshaw & Harris, 1987).

The peak and trough positions in the (reduced + inhibitor) *minus* reduced difference spectrum are 565 and 560 nm for the α-band and 432−433 nm and 423−424 nm in the Soret region. Although both *b*-type haems have been reported to contribute to the absorbance around 560 nm, only haem *b*-558 shows a sharp spectrum in this region (Koland et al., 1984; Lorence et al., 1986), which most likely points to spectral perturbation of this haem by *decyl*-aurachin D. It is reasonable to assume close proximity of the perturbed haem and the inhibitor binding site (Rich et al., 1990), which would also place the inhibitor site close to the proposed quinol domain near this haem (Dueweke & Gennis, 1990).

No spectral effects of *decyl*-aurachin D on reduced or oxygenated haem *d* were observed.

Addition of *decyl*-aurachin D from an ethanolic stock solution had no effect on the EPR spectrum of air-oxidized cytochrome *bd* at 10 or 50 K except for a line shape change of the $g = 6$ signal caused by the ethanol itself (not shown).

Kinetic Effects of Decyl-aurachin D. It has been shown (Meunier et al., 1995) that the related compound aurachin C, a potent inhibitor of both *bd* and *bo* type oxidases, acts not at the oxygen reduction site but at or near the quinol oxidation site of these enzymes. Analogous experiments were carried out to establish *decyl*-aurachin D as a quinol antagonist in cytochrome *bd*.

Optical changes in the Soret region (430 nm) were monitored during turnover with duroquinol. After addition of substrate, a period of steady-state turnover with partial haem reduction is observed (Figure 3). This is followed, on anaerobiosis, by full reduction of the haem groups. Although similar steady-state levels of haem reduction and oxygen intermediates are reached in the *decyl*-aurachin D containing sample, the approach to the steady-state following

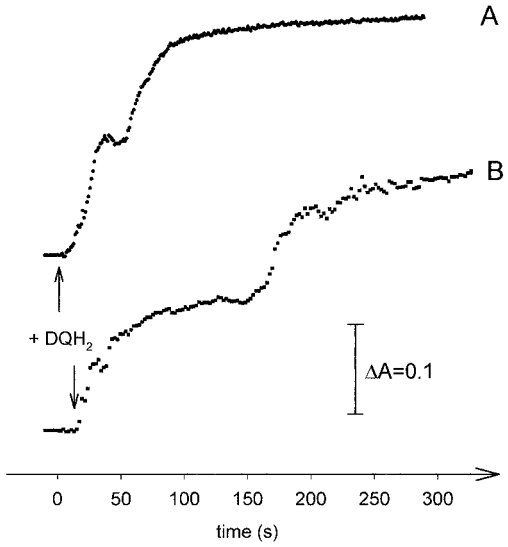

FIGURE 3: Effect of *decyl*-aurachin D on the steady-state behavior of cytochrome *bd*. Formation of turnover intermediates and haem reduction were recorded optically (at 430 nm) as described in Materials and Methods. Cytochrome *bd* (0.4 μM) was suspended in 50 mM potassium phosphate buffer, 1 mM EDTA, pH 7.5, containing 0.05% (w/v) lauryl maltoside. The substrate was 0.62 mM duroquinol: (A) control, (B) in presence of 2.5 μM *decyl*-aurachin D.

the initial quinol pulse is markedly inhibited. This suggests that *decyl*-aurachin D acts at the electron-input side of haem *b*-558.

In addition, CO recombination to dithionite-reduced cytochrome *bd* following flash photolysis is unaffected by *decyl*-aurachin D. Both the inhibited and the control samples show multiphasic CO binding with kinetic spectra and rate constants as reported previously (Jünemann et al., 1995b). In particular, for the phase due to CO binding to haem *d*, the present experiments give rate constants of $(1.5 \pm 0.1) \times 10^8$ and $(1.4 \pm 0.1) \times 10^8$ M^{-1} s^{-1} in the absence and presence of *decyl*-aurachin D, respectively (Figure 4). Also shown in Figure 4 is the effect of *decyl*-aurachin D on the CO recombination rate in mixed-valence enzyme which, in contrast to the dithionite-reduced system, is substantial.

Effect of Decyl-aurachin D on the Midpoint Potential of Haems b-558 and b-595. We have examined the effect of *decyl*-aurachin D on the midpoint potentials of haems *b*-558 and *b*-595 at pH 7.5. In the absence of *decyl*-aurachin D, titration of haem *b*-558, monitored at 562 nm with 546 and 580 nm as reference points, revealed two components with midpoint potentials of 60 ± 20 mV (10−30%) and 125 ± 10 mV (three measurements) assuming independent species with *n* values of 1 (Figure 5A). Haem *b*-595 titrated with an E_m of 175 ± 10 mV and haem *d* showed a midpoint potential of 245 ± 10 mV. The results are summarized in Table 1.

These values for *A. vinelandii* are within the range of values (136−195 mV for the *b*-type haems, 230−260 mV for haem *d*, at pH 7) reported for the *E. coli* enzyme (Pudek & Bragg, 1976; Lorence et al., 1984; Lorence et al., 1986; Meinhardt et al., 1989; Rothery & Ingledew, 1989). In these works, E_m(*b*-558) is generally higher than E_m(*b*-595). However, E_m(*b*-558) depends strongly on the composition of the hydrophobic phase, and values as low as 50−90 mV have been found in the presence of some detergents (Koland et al., 1984; Lorence et al., 1984; Green et al., 1986).

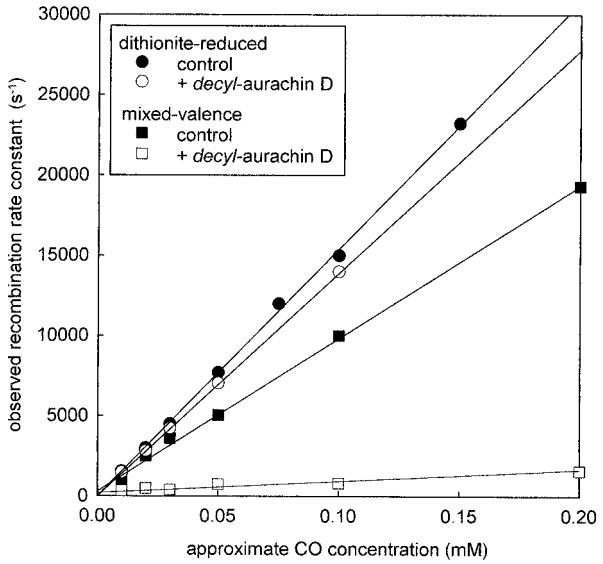

FIGURE 4: Rates of CO recombination following flash photolysis of the dithionite and mixed-valence CO compounds of cytochrome *bd* in the absence and presence of d*ecyl*-aurachin D. Cytochrome *bd* (2 μM) was suspended in 50 mM potassium phosphate buffer (pH 7.5) containing 1 mM EDTA and 0.05% (w/v) lauryl maltoside. CO was added to the dithionite-reduced or the mixed-valence enzyme (prepared as in Figure 6) from CO-saturated water. *Decyl*-aurachin D was added to a final concentration of 6 μM. Recombination rates were derived from transients taken at 622, 634, and 642 nm, with a dark time of 1 s and 25 averages per wavelength.

Table 1: Midpoint Potentials at pH 7.5 of Cytochrome *bd* in the Absence and Presence of *Decyl*-aurachin D[a]

	$E_{m7.5}$ (mV)	
haem	control sample	+ *decyl*-aurachin D
b-558	60 ± 20 (10−30%)	90 ± 20 (30%)
	125 ± 10	189 ± 10
b-595	175 ± 10	135 ± 10
d	245 ± 10	240 ± 10

[a] Conditions were as in Figure 5.

While the midpoint potential of haem *d* is unaffected by *decyl*-aurachin D (Figure 5B), the E_m values of both *b*-type haems are shifted in the presence of 6 μM *decyl*-aurachin D (3-fold molar excess), to 189 ± 10 mV for haem *b*-558 (30% low-potential component at 90 ± 20 mV) and 135 ± 10 mV for haem *b*-595 (Figure 5B). Hence, in the presence of *decyl*-aurachin D, the midpoint potential of haem *b*-558 increases whereas E_m(*b*-595) decreases to a value lower than E_m(*b*-558).

Preparation of the Mixed-Valence, CO-Ligated Form of Cytochrome bd. The major species in "as prepared" cytochrome *bd* is the one-electron reduced form where oxygen is reversibly bound to haem *d*, giving rise to a characteristic absorbance band near 650 nm (Poole et al., 1983; Lorence & Gennis, 1989). Figure 6B shows that on deoxygenation of the sample this absorbance band disappears, and a signal at 630 nm forms, due to ferrous haem *d*. Almost no *b*-haem reduction is observed. The one-electron reduced form can bind CO to give a ($b^{3+}b^{3+}d^{2+}$-CO) species whose absorbance band at 636 nm is at the same position as in the fully ferrous CO-ligated enzyme, although broader and less intense ((Kauffman et al., 1980) and Figure 6). The other components in "as prepared" enzyme, oxoferryl and ferric species, together typically comprising less than 30% of the preparation (Lorence & Gennis, 1989; Krasnoselskaya et al., 1993;

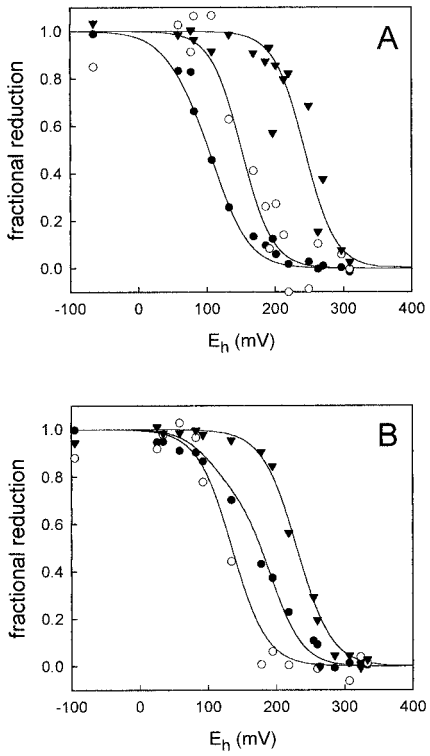

FIGURE 5: Redox titrations of cytochrome *bd* in absence and presence of *decyl*-aurachin D. Redox titrations were performed using approximately 2 μM cytochrome *bd* in 50 mM potassium phosphate, 1 mM EDTA, 0.05% (w/v) lauryl maltoside, pH 7.5. The data represent points taken in both the oxidative and reductive direction. The reduction level of the haems was monitored by triple wavelength measurements as described in Materials and Methods: (A) control; (B) plus 6 μM *decyl*-aurachin D. The individual haems are represented by open circles (*b*-558), filled circles (*b*-595), and triangles (*d*). The experimental data are overlayed with simulated titration curves using the following parameters (all independent "n = 1" species): (A) *b*-558, E_{m1} = 70 mV (15%) and E_{m2} = 120 mV; *b*-595, E_m = 170 mV; *d*, E_m = 245 mV. (B) *b*-558, E_{m1} = 90 mV (30%) and E_{m2} = 189 mV; *b*-595, E_m = 135 mV; *d*, E_m = 240 mV.

Jünemann & Wrigglesworth, 1995), would be unreactive toward deoxygenation and treatment with CO. When *decyl*-aurachin D is present, the spectrum of deoxygenated cytochrome *bd* shows some reduction of both *b*-type haems, indicative of altered redox potentials. At the same time, the 630 nm feature is much decreased. The *b*-haems reoxidize when CO is added to the *decyl*-aurachin D-bound sample, showing the formation of the same mixed-valence CO compound as in the control without inhibitor.

Reversed Electron Transfer. The mixed valence CO compound of cytochrome *bd* is photolyzable and shows a kinetic spectrum consistent with generation of the unligated ferrous haem *d*. However, the rate constant for CO recombination to the mixed-valence enzyme is about 60% of that seen with the fully reduced enzyme, $(1 \pm 0.1) \times 10^8$ compared to $(1.5 \pm 0.1) \times 10^8$ M^{-1} s^{-1} (Figure 4).

It can be expected that some electron redistribution occurs after photolysis of the mixed valence CO compound, as seen from the relative E_ms and from the static spectrum of the unligated, one-electron reduced form, and that this electron redistribution should be increased by *decyl*-aurachin D.

In a sample containing *decyl*-aurachin D, the following processes are observed following photolysis (Figures 7 and 8A):

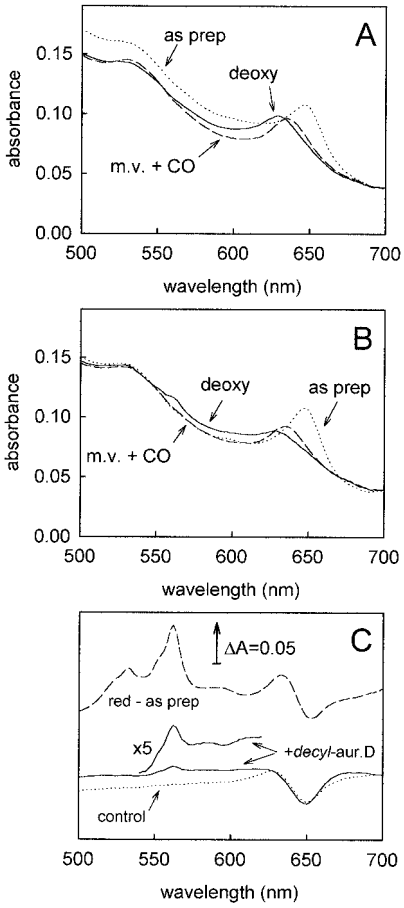

FIGURE 6: Optical spectra of deoxygenated and mixed-valence, CO-ligated cytochrome *bd* in the absence and presence of *decyl*-aurachin D. Cytochrome *bd* (2 μM) in 50 mM potassium phosphate, 1 mM EDTA, 0.05% (w/v) lauryl maltoside, pH 7.5, was deoxygenated with glucose/glucose oxidase/catalase as described in Materials and Methods. The sample was judged to be anaerobic when the 650 nm band of oxygenated cytochrome *d* had completey disappeared. CO (4 μM) was added to the deoxygenated sample from CO-saturated water to generate the mixed valence CO compound of cytochrome *bd*. A low CO concentration at which binding would still be stoichiometric was chosen in order to lower the recombination rate in the kinetic experiment (Figures 7 and 8). To ensure anaerobiosis and exclude competition with oxygen, the sample was left for 2−3 min before recording the spectrum of the mixed-valence CO compound of cytochrome *bd*. *Decyl*-aurachin D was added before deoxygenation or introduction of CO to a final concentration of 6 μM, as indicated. The figure shows "as prepared", deoxygenated, and mixed-valence, CO-ligated enzyme in absence (A) and presence (B) of *decyl*-aurachin D. Deoxygenated *minus* "as prepared" difference spectra are given in (C). For comparison, the dithionite-reduced *minus* "as prepared" difference spectrum is also included in panel C.

1. Immediately after the flash (0.088 ms) the unligated one-electron-reduced form of cytochrome *bd* is formed. This can be seen as a rise in absorbance in the transient at 623 nm (Figure 7A) and a loss in absorbance at around 640 nm (not shown) or at 562 nm (Figure 7C). The kinetic spectrum of this phase can be interpreted as the ($b^{3+}b^{3+}d^{2+}$) *minus* ($b^{3+}b^{3+}d^{2+}$-CO) difference spectrum.

2. This is followed within a millisecond (at a rate of 3000 s^{-1}) by simultaneous decay of the 623 nm peak of ferrous haem *d* (*without* relaxation of the 644 nm trough due to d^{2+}-CO, Figure 8A) and appearance of a signal around 560 nm. The kinetics of this phase can be most clearly seen at 634 nm, which is close to an isosbestic point for CO rebinding to ferrous haem *d* (Figures 7B and 8A). We attribute this

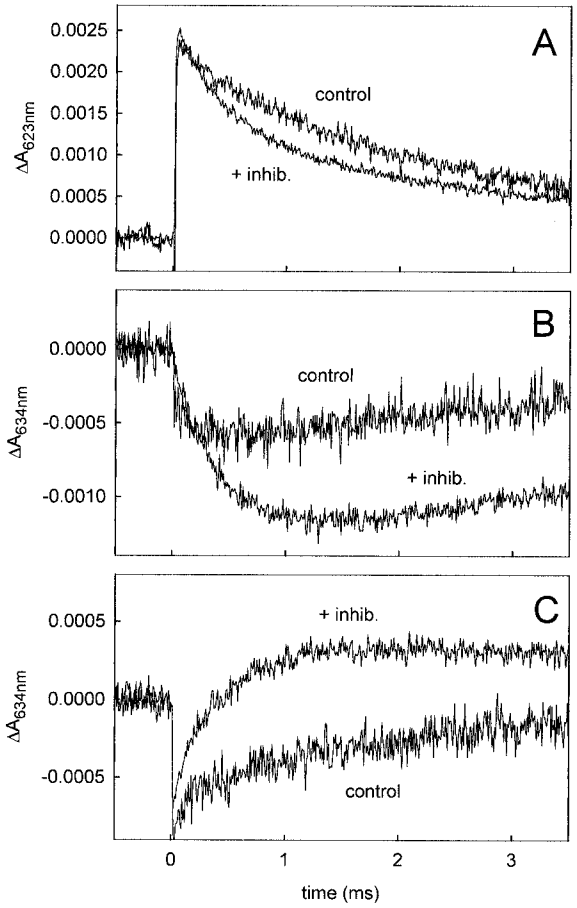

FIGURE 7: Effect of *decyl*-aurachin D on the rates of internal electron redistribution and CO recombination following flash photolysis of the mixed-valence CO compound of cytochrome *bd*. Transients shown are at (A) 623 nm, near the peak postition of ferrous haem *d* in the postphotolysis spectrum (B) 634 nm, close to the isosbestic point for free and CO ligated mixed valence enzyme, and (C) 562 nm, monitoring *b*-558. In order to minimize flash artefacts, narrow filtering was used with windows of (A) 600 ± 20 nm, (B) nm 631 ± 11 nm, and (C) 561 ± 8.6 nm. Traces were normalized to give identical amplitudes based on the initial photolyzed product (623 nm). Twenty-five averages per wavelength were recorded with a dark time between flashes of 1 s. Generation of mixed valence CO-ligated cytochrome *bd* and other conditions were as in Figure 6.

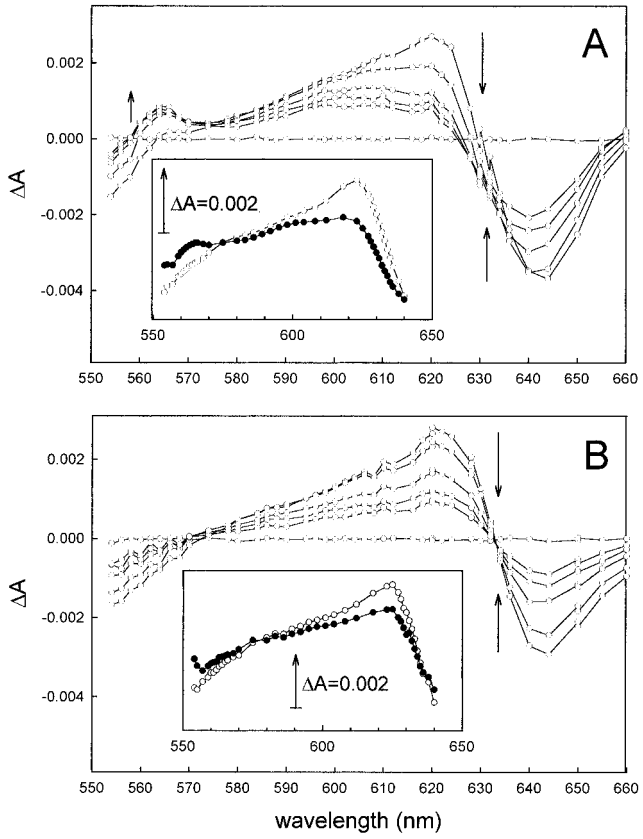

FIGURE 8: Kinetic spectra of internal electron redistribution and CO recombination following flash photolysis of the mixed valence CO compound of cytochrome *bd*. Kinetic spectra were calculated from transients taken cyclically at individual wavelengths. The photomultiplier was protected with a 550 nm cut-on filter. The spectra shown are at 0.28, 0.66, 1.088, 2.58, and 3.54 ms after the flash, together with the preflash baseline. The insets show spectra at 0.088 ms after the flash and at the plateau of the fast phase of electron-redistribution (1.088 ms). These spectra are combined data of three individual experiments using filtering as in Figure 7. Generation of the mixed-valence CO compound at 4 μM CO and other conditions were as in Figures 6 and 7: (A) in the presence of 6 μM *decyl*-aurachin D, (B) control.

phase to oxidation of haem *d*, which in its ferric form shows little absorbance in the visible region, and reduction of haem *b*-558. Electron back-donation to haem *b*-595 could not be assessed due to the low extinction coefficient of this haem (compare Figure 6C, signal around 596 nm) and its overlap with changes of haem *d*. The kinetic spectrum in the Soret region has a peak at 432−436 nm and a trough near 418 nm (not shown), again consistent with the reduction of some *b*-type haem.

3. Lastly, the system in this phase relaxes back to the mixed-valence CO compound with an observed rate constant of 400 s^{-1} at 4 μM CO, at all wavelengths.

The behavior of the control sample without inhibitor is shown in Figures 7 and 8B. As in the *decyl*-aurachin D-inhibited sample, the first kinetic spectrum following the flash (0.088 ms) corresponds to formation of the species ($b^{3+}b^{3+}d^{2+}$). The second phase, oxidation of haem *d* with concomitant reduction of a *b*-type haem, is small, as expected from the static spectra and the relative midpoint potentials. Close inspection of the transients at 634 and 562 nm (Figure 7B,C) reveals some of this redox phase within the first 0.2−0.3 ms after the flash, but the small signal amplitude of this phase does not allow the determination of an electron redistribution rate. Relaxation to the ($b^{3+}b^{3+}d^{2+}$-CO) species then occurs, again with an observed rate constant of 400−500 s^{-1} at 4 μM CO. It should be noted, however, that at increasing CO concentrations the observed rate of recombination is markedly lower in the *decyl*-aurachin D-inhibited sample (Figure 4), giving an apparent bimolecular rate constant of (0.6 ± 0.05) × 10^7, compared to (1 ± 0.1) × 10^8 M^{-1} s^{-1} in the control. This difference can be partly explained by the lowered concentration of the actual CO binding species, d^{2+}, in the inhibited sample where a large proportion of haem *d* has transiently been oxidized because of the reversed electron transfer to the haems *b*. However, the changes in rate constant were larger (about 17-fold decrease) than can be accounted for solely by haem *d* oxidation (estimated 30%, see below). Hence, some other effect must be involved. A general conformational change induced by *decyl*-aurachin D binding is unlikely to be involved since the CO recombination rate constant in fully reduced enzyme is essentially unaltered by the inhibitor (Figure 4). Also, in the uninhibited mixed-valence sample, the rate constant of CO recombination is only about 60% of

that in the fully reduced (uninhibited) enzyme (Figure 4), although very little electron backflow is observed. Thus, a simple model where the rate constant is largely determined by the level of ferrous haem d^{2+} would not be sufficient, and further work is needed to study the behavior of the oxygen binding site in the mixed-valence state.

DISCUSSION

Redox Potentials. Redox titrations of the low-spin haem *b* component of our preparation of cytochrome *bd*, recorded at 560 nm with 546 and 580 nm as reference wavelengths, reveal a biphasic curve. This can be fitted assuming two independent "$n = 1$" species with midpoint potentials of 50−70 and 120−130 mV, the former comprising up to 30% of the total signal. This biphasicity may have various causes, including redox interaction of the *b*-type haems, redox interaction with an unseen species such as a quinone, or heterogeneity of the preparation. Redox interaction between the *b*-type haems in cytochrome *bd* from *E. coli* has not been noted previously, with the exception of Meinhardt *et al.* (1989) who reported *b*-595/*d* interaction. If the biphasicity of the redox titration curve is due to interaction with a quinone, it could be expected that it might be abolished if the interacting quinone is replaced by *decyl*-aurachin D, a case similar to the behavior of the bc_1 complex in presence of Q_i site inhibitors (Rich et al., 1990). Although a return to a monophasic titration in the presence of the inhibitor is not observed here, interaction with a quinone cannot be entirely ruled out since not enough is known about the number and nature of the Q-site(s) in the enzyme. The present redox titration data have been analyzed assuming independent $n = 1$ species with heterogeneity as the most likely cause of the biphasicity. This interpretation is strengthened by the observation that the amount of the low potential component increases as the sample ages. Formation of a lower potential species might arise because of loss of the more labile methionine axial ligand of haem *b*-558 (Kaysser et al., 1995; Spinner et al., 1995). This heterogeneity in haem *b*-558 would not appear to be reflected in the oxygen binding site since the CO recombination kinetics to haem *d*, a parameter likely to be very sensitive to small structural changes, remain monophasic.

Internal Electron Transfer. Room temperature internal electron transfer in cytochrome *bd* has been studied previously using the flow-flash technique (Hill et al., 1994). After photolysis of carbon monoxide from the fully reduced enzyme, oxygen first reacted in a second-order process with a rate constant of 2×10^9 M^{-1} s^{-1} to form a ferrous haem *d*−oxygen adduct. This was followed by internal electron transfer reactions, all with a rate constant of 10^4 s^{-1}, in which all three haems became oxidized and an oxyferryl form of haem *d* was produced.

Reversed electron transfer after photolysis of carbon monoxide from the mixed-valence form of the enzyme offers an alternative method to study internal electron transfer and has been used extensively with cytochrome *c* oxidase and cytochrome *bo* [reviewed in Einarsdóttir (1995)]. This technique is potentially also applicable to cytochrome *bd* since a mixed valence compound can be formed in which haem *d i*s reduced with carbon monoxide bound and both haems *b* are oxidized (Figure 6). However, because unligated haem *d* ($E_m^{7.5} = 245$ mV) has a significantly higher midpoint potential than the haems *b* ($E_m^{7.5}$ of 125 and 175 mV, respectively), very little reversed electron transfer to the *b*-type haems is expected to occur after the carbon monoxide has been photolyzed, as was observed to be the case (Figure 7). However, binding of *decyl*-aurachin D alters the relative midpoint potentials of the haem groups in favor of more extensive reversed electron transfer, as shown in Figures 5 and 7.

In the data of the inset of Figure 8A, we may estimate from the first kinetic spectrum taken at 88 μs that approximately 260 nM haem d^{2+}-CO was photolyzed to unligated haem d^{2+} (using an extinction coefficient of 18 mM^{-1} cm^{-1} at 623−643 nm for the (reduced *plus* CO) *minus* reduced difference spectrum (Jünemann & Wrigglesworth, 1995)). Subsequently, in the reversed electron transfer phase which occurs within the next 1 ms, approximately 60% of the peak due to ferrous haem d^{2+} is lost due both to reversed electron transfer and, partially, to recombination of carbon monoxide. From the control data (inset to Figure 8B) the recombination with CO accounts for about 30% of the peak loss. Hence, 30% (75 nM) of the ferrous haem *d* was oxidized due to reversed electron transfer. This is accompanied by reduction of approximately 50 nM of haem *b*-558 (using an extinction coefficient of about 20 mM^{-1} cm^{-1} at 558−580 nm for its reduced *minus* oxidized difference spectrum (Green et al., 1986)). The remaining 25 nM reducing equivalents are likely to have appeared on the high spin haem *b*-595, although this is difficult to ascertain directly from the spectra because of its indistinct spetrum and its overlap with other components. Although approximate, this rough analysis does indeed suggest that the postphotolysis redistribution of electrons between the haem groups is consistent with their estimated midpoint potentials and that it is the effects of *decyl*-aurachin D on these midpoint potentials which has increased the reversed electron transfer to a level that is easily monitored.

The rate constant of 3000 s^{-1} for this internal redistribution is also generally consistent with the value of 10^4 s^{-1} observed previously for forward electron transfer in the more thermodynamically favorable direction (Hill et al., 1994) and with the maximum turnover number of the enzyme at (pH 7.9) of around 4000 electons s^{-1} (Jünemann et al., 1995a).

Site of Inhibition by Decyl-aurachin D. The present experiments show that *decyl*-aurachin D does not directly affect the oxygen binding site of cytochrome *bd*. Although *decyl*-aurachin D did inhibit the approach to steady-state haem reduction levels following a quinol pulse, similar levels of steady-state reduction of the *b*-type haems were reached in the control and inhibited samples following the pulse. The rate of CO binding to haem *d* in fully ferrous cytochrome *bd* was not inhibited. Hence, inhibition must occur by interference with quinol binding and/or electron transport from quinol to the initial intrinsic electron acceptor (*b*-558). The spectral changes induced by binding of *decyl*-aurachin D to fully-reduced cytochrome *bd* can be attributed to perturbation of haem *b*-558, located close to the proposed quinol oxidase domain (Dueweke & Gennis, 1991), and support the idea that the compound binds at or near this site. The inhibitor-induced E_m shift of haem *b*-558, with no effect on $E_m(d)$, is a further indication of this close proximity.

Part of the quinolone structure of *decyl*-aurachin D closely resembles the structure of the substrate quinol, suggesting that the inhibitor could bind directly to the quinol oxidation site in cytochrome *bd*. The lack of inhibition of the TMPD

oxidase activity at concentrations sufficient to inhibit quinol oxidation by 95% can be seen as supporting this view since TMPD has been shown to operate *via* a different electron entry site than quinol (Kranz & Gennis, 1984; Lorence et al., 1988; Dueweke & Gennis, 1991). Furthermore, reversed electron transfer in the *decyl*-aurachin D-containing sample is still too fast, at approximately 3000 s^{-1}, to account for the inhibition. As discussed above, the increased amplitude of electron backflow in unligated, *decyl*-aurachin D-inhibited enzyme can be explained by the E_m shift of the *b*-type haems, in particular the marked decrease of $\Delta(E_m(b\text{-}558)-E_m(d))$. The lack of inhibition of the TMPD oxidase activity suggests that the *decyl*-aurachin D-induced effect on the midpoint potential of haem *b*-558 is not the cause of inhibtion of quinol oxidation, but a secondary effect resulting from binding of the inhibitor at a nearby site. The decrease of E_m(*b*-595) may be a tertiary effect due to a disrupted interaction with haem *b*-558.

The proposal that *decyl*-aurachin D acts at the catalytic quinol binding site seems to be difficult to reconcile with a noncompetitive type of inhibition. The possibility must be entertained that systems containing hydrophobic and aqueous phases can diverge from ideal solution behavior, and this might distort conventional enzyme kinetic plots and their interpretation. However, in a recent study on quinol antagonists in the *bo*-type oxidase from *E. coli*, Musser and co-workers showed for short-chain ubiquinols that deviations from ideal behavior are not greater than 20−30%, thus still allowing a classical enzymological approach (Musser et al., 1997). Nevertheless, such deviations from ideal behavior will depend on conditions of temperature, detergent, and lipid concentrations and should not be ruled out completely at this stage.

Furthermore, plots showing a noncompetitive type of inhibition can arise from several mechanisms. For example, the inhibitor may bind to the active site as a product (quinone) analogue to a form of the enzyme which differs (e.g. in redox or oxygenation state) from the form binding the quinol substrate (Cornish-Bowden, 1995), and more rigorous investigations would be required to assess such possbilities.

A further type of explanation could arise from the presence of more than one binding site for quinones, a situation that has been suggested for several other systems, including mitochondrial and bacterial complexes I and III (Brandt et al., 1988; Friedrich et al., 1994a,b; Ding et al., 1992, 1995) and the *bo*-type oxidase from *E. coli* (Musser et al., 1997) which contains a strongly-bound ubiquinol in addition to the substrate quinol (Sato-Watanabe et al., 1994). Although most of the evidence to date is compatible with there being only one binding site for quinones in the quinol oxidation site in cytochrome *bd* (see review in (Jünemann, 1997)), this possibility cannot be excluded at present.

Despite these uncertainties, our data show conclusively that *decyl*-aurachin D acts on the donor side of haem *b*-558, preventing electron donation into the enzyme from quinol substrate, without substantially affecting internal electron transfer rates or the oxygen reduction site.

ACKNOWLEDGMENT

We thank Susan Hill (University of Sussex) for large-scale growth of *A. vinelandii* cells and Richard Cammack (King's College London) for use of the EPR spectrometer.

REFERENCES

Bagshaw, C. R., & Harris, D. A. (1987) in *Spectrophotometry and spectrofluorimetry: a practical approach* (Bashford, C. L., & Harris, D. A., Eds.) pp 91−113, IRL, Oxford.
Brandt, U., Schägger, H., & von Jagow, G. (1988) *Eur. J. Biochem. 173*, 499−506.
Cornish-Bowden, A. (1995) in *Fundamentals of Enzyme Kinetics*, Portland Press, London.
D'mello, R., Palmer, S., Hill, S., & Poole, R. K. (1994) *FEMS Microbiol. Lett. 121*, 115−120.
Ding, H., Robertson, D. E., Daldal, F., & Dutton, P. L. (1992) *Biochemistry 31*, 3144−3158.
Ding, H., Moser, C. C., Robertson, D. E., Tolito, M. K., Daldal, F., & Dutton, P. L. (1995) *Biochemistry 34*, 15979−15996.
Dixon, M. (1972) *Biochem. J. 129*, 197−202.
Dueweke, T. J., & Gennis, R. B. (1990) *J. Biol. Chem. 265*, 4273−4277.
Dueweke, T. J., & Gennis, R. B. (1991) *Biochemistry 30*, 3401−3406.
Dutton, P. L., & Wilson, D. F. (1974) *Biochim. Biophys. Acta 346*, 165−212.
Einarsdóttir, O. (1995) *Biochim. Biophys. Acta 1229*, 129−147.
Fang, H., Lin, R., & Gennis, R. B. (1989) *J. Biol. Chem. 264*, 8026−8032.
Friedrich, T., Ohnishi, T., Forche, E., Kunze, B., Jansen, R., Trowitzsch, W., Höfle, G., Reichenbach, H., & Weiss, H. (1994a) *Biochem. Soc. Trans. 22*, 226−230.
Friedrich, T., Van Heek, P., Leif, H., Ohnishi, T., Forche, E., Kunze, B., Jansen, R., Trowitzsch-Kienast, W., Höfle, G., Reichenbach, H., & Weiss, H. (1994b) *Eur. J. Biochem. 219*, 691−698.
Green, G. N., Lorence, R. M., & Gennis, R. B. (1986) *Biochemistry 25*, 2309−2314.
Henderson, P. J. F. (1972) *Biochem. J. 127*, 321−333.
Hill, B. C., Hill, J. J., & Gennis, R. B. (1994) *Biochemistry 33*, 15110−15115.
Hill, J. J., Alben, J. O., & Gennis, R. B. (1993) *Proc. Natl. Acad. Sci. U.S.A. 90*, 5863−5867.
Jünemann, S. (1997) *Biochim. Biophys. Acta* (in press).
Jünemann, S., & Wrigglesworth, J. M. (1994) *FEBS Lett. 345*, 198−202.
Jünemann, S., & Wrigglesworth, J. M. (1995) *J. Biol. Chem. 270*, 16213−16220.
Jünemann, S., Butterworth, P. J., & Wrigglesworth, J. M. (1995a) *Biochemistry 34*, 14861−14867.
Jünemann, S., Rich, P. R., & Wrigglesworth, J. M. (1995b) *Biochem. Soc. Trans. 23*, 157S.
Kauffman, H. F., van Gelder, B. F., & Dervartanian, D. V. (1980) *J. Bioenerg. Biomemb. 12*, 265−276.
Kaysser, T. M., Ghaim, J. B., Georgiou, C., & Gennis, R. B. (1995) *Biochemistry 34*, 13491−13501.
Kelly, M. J. S., Poole, R. K., Yates, M. G., & Kennedy, C. (1990) *J. Bacteriol. 172*, 6010−6019.
Kita, K., Konishi, K., & Anraku, Y. (1984) *J. Biol. Chem. 259*, 3375−3381.
Koland, J. G., Miller, M. J., & Gennis, R. B. (1984) *Biochemistry 23*, 1051−1056.
Kolonay, J. F.,Jr., Moshiri, F., Gennis, R. B., Kaysser, T. M., & Maier, R. J. (1994) *J. Bacteriol. 176*, 4177−4181.
Konishi, K., Ouchi, M., Kita, K., & Horikoshi, I. (1986) *J. Biochem. 99*, 1227−1236.
Kranz, R. G., & Gennis, R. B. (1984) *J. Biol. Chem. 259*, 7998−8003.
Kranz, R. G., & Gennis, R. B. (1985) *J. Bacteriol. 161*, 709−713.
Krasnoselskaya, I., Arutjunjan, A. M., Smirnova, I., Gennis, R., & Konstantinov, A. A. (1993) *FEBS Lett. 327*, 279−283.
Lorence, R. M., & Gennis, R. B. (1989) *J. Biol. Chem. 264*, 7135−7140.
Lorence, R. M., Miller, M. J., Borochov, A., Faiman-Weinberg, R., & Gennis, R. B. (1984) *Biochim. Biophys. Acta 790*, 148−153.
Lorence, R. M., Koland, J. G., & Gennis, R. B. (1986) *Biochemistry 25*, 2314−2321.
Lorence, R. M., Carter, K., Gennis, R. B., Matsushita, K., & Kaback, H. R. (1988) *J. Biol. Chem. 263*, 5272−5276.

Meinhardt, S. W., Matsushita, K., Kaback, H. R., & Ohnishi, T. (1989) *Biochemistry 28*, 2153−2160.
Meunier, B., Madgwick, S. A., Reil, E., Oettmeier, W., & Rich, P. R. (1995) *Biochemistry 34*, 1076−1083.
Miller, M. J., & Gennis, R. (1983) *J. Biol. Chem. 258*, 9159−9165.
Moshiri, F., Chawla, A., & Meier, R. J. (1991) *J. Bacteriol. 173*, 6230−6341.
Musser, S. M., Stowell, M. H. B., Lee, H. K., Rumbley, J. N., & Chan, S. I. (1997) *Biochemistry 36*, 894−902.
Oettmeier, W., Masson, K., Soll, M., & Reil, E. (1994) *Biochem. Soc. Trans. 22*, 213−216.
Poole, R. K., Kumar, C., Salmon, I., & Chance, B. (1983) *J. Gen. Microbiol. 129*, 1335−1344.
Pudek, M. R., & Bragg, P. D. (1976) *Arch. Biochem. Biophys. 174*, 546−552.
Reil, E., Soll, M., Masson, K., & Oettmeier, W. (1994) *Biochem. Soc. Trans. 22*, 62S.
Rich, P. R. (1981) *Biochim. Biophys. Acta 637*, 28−33.
Rich, P. R., Jeal, A. E., Madgwick, S. A., & Moody, A. J. (1990) *Biochim. Biophys. Acta 1018*, 29−40.
Rothery, R. A., & Ingledew, W. J. (1989) *Biochem. J. 261*, 437−443.
Sato-Watanabe, M., Mogi, T., Ogura, T., Kitagawa, T., Miyoshi, H., Iwamura, H., & Anraku, Y. (1994) *J. Biol. Chem. 269*, 28908−28912.
Smith, A., Hill, S., & Anthony, C. (1990) *J. Gen. Microbiol. 136*, 171−180.
Spinner, F., Cheesman, M. R., Thomson, A. J., Kaysser, T., Gennis, R. B., Peng, Q., & Peterson, J. (1995) *Biochem. J. 308*, 641−644.
Takamiya, K., & Dutton, P. L. (1979) *Biochim. Biophys. Acta 546*, 1−16.
von Jagow, G., & Link, T. A. (1986) *Methods Enzymol. 126*, 253−271.

BI970055M